

Angular momentum projected analysis of Quadrupole Collectivity in $^{30,32,34}\text{Mg}$ and $^{32,34,36,38}\text{Si}$ with the Gogny interaction.

R. Rodríguez-Guzmán, J.L. Egido and L.M. Robledo.

*Departamento de Física Teórica C-XI, Universidad Autónoma de Madrid, 28049
Madrid, Spain*

Abstract

A microscopic angular momentum projection after variation is used to describe quadrupole collectivity in $^{30,32,34}\text{Mg}$ and $^{32,34,36,38}\text{Si}$. The Hartree-Fock-Bogoliubov states obtained in the quadrupole constrained mean field approach are taken as intrinsic states for the projection. Excitation energies of the first 2^+ states and the $B(E2, 0^+ \rightarrow 2^+)$ transition probabilities are given. A reasonable agreement with available experimental data is obtained. It is also shown that the mean field picture of those nuclei is strongly modified by the projection.

Key words:

PACS: 21.60.Jz, 21.60.-n, 21.10.Re, 21.10.Ky, 21.10.Dr, 27.30.+t

Neutron-rich nuclei with $N \approx 20$ are spectacular examples of shape coexistence between spherical and deformed states. Experimental evidence for an island of deformed nuclei near $N = 20$ has been found in the fact that ^{31}Na and ^{32}Na are more tightly bound than could be explained with spherical shapes [1]. Additional support comes from the unusually low excitation energy of the 2^+ state in ^{32}Mg [2]. A large ground state deformation has also been inferred from intermediate energy Coulomb excitation studies [3] in ^{32}Mg . Quadrupole collectivity of $^{32-38}\text{Si}$ has also been studied in [4]. Very recently this region has been the subject of detailed experimental spectroscopic studies at ISOLDE [5]. From a theoretical point of view, deformed ground states have been predicted for nuclei with $N \approx 20$ [6–8]. In those calculations the rotational energy correction is the essential ingredient for the stabilization of the deformed configuration. On the other hand, some calculations have predicted [9–12] a spherical ground state for ^{32}Mg but it has also been found [12] that deformation effects may appear as a result of dynamical correlations. Some shell model calculations, even with restricted configuration spaces, have

been able to explain the increased quadrupole collectivity at $N = 20$ as a result of neutron $2p - 2h$ excitations into the fp shell, see for example [13,14]. Recently, a mean field study has explored the suitability of several Skyrme parameterizations [15] in the description of this and other regions of shape coexistence.

The mean field description of nuclei is usually a good starting point as it provides a qualitative, and in many cases quantitative, understanding of the nuclear properties. This is the case when the mean field solution corresponds to a well defined minimum. However, in regions of shape coexistence where two minima are found at a comparable energy, the correlation effects stemming from the restoration of broken symmetries and/or collective motion can dramatically alter the energy landscape thus changing the mean field picture. For this reason, we have included in our mean field calculations the effects related to the restoration of the broken rotational symmetry by performing, for the first time with the Gogny force, angular momentum projected calculations of the energies and other relevant quantities. The reason for choosing to restore rotational symmetry is that the zero point energy associated with this restoration is somehow proportional to deformation and ranges, in this region, from a few KeV for nearly spherical configurations to several MeV for well deformed ones. This energy range is comparable to the energy differences found between different shapes in nuclei of this region. Therefore, in addition to the mean field results, both angular momentum projected $I = 0$ and $I = 2$ surfaces were computed for the nuclei $^{30,32,34}\text{Mg}$ and $^{32,34,36,38}\text{Si}$ and angular momentum projected transition probabilities $B(E2, 0^+ \rightarrow 2^+)$ among different configurations.

The calculation proceeds in two steps: in the first one we perform a set of constrained Hartree- Fock- Bogoliubov (HFB) calculations using the D1S parameterization [16] of the Gogny force [17] and the mass quadrupole operator $\hat{Q}_{20} = z^2 - \frac{1}{2}(x^2 + y^2)$ as the constraining operator in order to obtain a set of “intrinsic” wave functions $|\phi(q_{20})\rangle$. The self-consistent symmetries imposed in the calculation were axial symmetry, parity and time reversal. The two body kinetic energy correction was fully taken into account in the minimization process. On the other hand, the Coulomb exchange term was replaced by the local Slater approximation and neglected in the variational process. The Coulomb pairing term as well as the contribution to the pairing field from the spin-orbit interaction were neglected. A harmonic oscillator (HO) basis of 10 major shells was used to expand the quasi-particle operators and the two oscillator lengths defining the axially symmetric HO basis were kept equal for all the values of the quadrupole moment. The reason for choosing the basis this way was that we wanted a basis closed under rotations (i.e. an arbitrary rotation of the basis elements always yields wave functions that can be solely expressed as linear combinations of the elements of the basis) in order to avoid the technical difficulties discussed in [18] when a non-closed basis is used. In

the second step we compute the angular momentum projected energy for each intrinsic wave function $|\phi(q_{20})\rangle$ obtaining in this way a set of energy curves $E_I(q_{20})$ for each value of $I = 0, 2, \dots$. The minima of each curve provide us with the energies and wave functions of the $I = 0^+, 2^+, \dots$ yrast and isomeric states.

The theoretical background for angular momentum projection is very well described in [19,20] and therefore we will not dwell on the details here. However, a few remarks concerning the peculiarities of our calculation are in order: first, and due to the axial symmetry imposed in the HFB wave functions, the angular momentum projected energy is given by

$$E_I(q_{20}) = \frac{\int_0^{\frac{\pi}{2}} d\beta \sin\beta d_{00}^I(\beta) \langle \phi(q_{20}) | \hat{H}'[\rho_\beta(\vec{r})] e^{-i\beta \hat{J}_y} | \phi(q_{20}) \rangle}{\int_0^{\frac{\pi}{2}} d\beta \sin\beta d_{00}^I(\beta) \langle \phi(q_{20}) | e^{-i\beta \hat{J}_y} | \phi(q_{20}) \rangle} \quad (1)$$

with $\hat{H}'[\rho_\beta(\vec{r})] = \hat{H}[\rho_\beta(\vec{r})] - \lambda_\pi(\hat{N}_\pi - Z) - \lambda_\nu(\hat{N}_\nu - N)$. The term $-\lambda_\pi(\hat{N}_\pi - Z) - \lambda_\nu(\hat{N}_\nu - N)$ is included to account for the fact that the projected wave function does not have the right number of particles on the average. The previous term would correspond to the application of first order perturbation theory if the chemical potentials used were the derivatives of the projected energy with respect to the number of particles. In our calculations we have simply used the chemical potentials obtained in the HFB theory¹. This simplification is justified by the fact that the deviations induced in the number of particles due to the angular momentum projection are always small and so are their effects on the projected energies.

For the computation of the matrix elements of the rotation operator in a HO basis we have used the results of ref. [21].

Another relevant point to be discussed is the prescription to use for the density dependent part of the Gogny force. In the calculation of the energy functional $E[\phi] = \langle \phi | \hat{H} | \phi \rangle$ the density appearing in the density dependent part of the force is simply $\rho(\vec{r}) = \langle \phi | \hat{\rho} | \phi \rangle$ rendering the energy a functional of the density and the pairing tensor but with a dependence on the density different from the canonical quadratic one of the standard HFB theory. On the other hand, the energy overlap $E[\phi, \phi'] = \langle \phi | \hat{H} | \phi' \rangle / \langle \phi | \phi' \rangle$ can be evaluated using the extended Wick theorem. The final expression is the same as the HFB functional $E[\phi]$ but replacing the density matrix by $\bar{\rho}_{ij} = \langle \phi | c_j^\dagger c_i | \phi' \rangle / \langle \phi | \phi' \rangle$ and the pairing tensor by $\bar{\kappa}_{ij} = \langle \phi | c_j c_i | \phi' \rangle / \langle \phi | \phi' \rangle$ and $\bar{\tilde{\kappa}}_{ij} = \langle \phi | c_i c_j | \phi' \rangle / \langle \phi | \phi' \rangle$. As a consequence, it seems rather natural to use the density $\bar{\rho}(\vec{r}) = \langle \phi | \hat{\rho} | \phi' \rangle / \langle \phi | \phi' \rangle$

¹ This recipe has been previously used [22] in the context of angular momentum projection and in Generator Coordinate Method (GCM) calculations [23]. In both cases it has been found that the present recipe works very well.

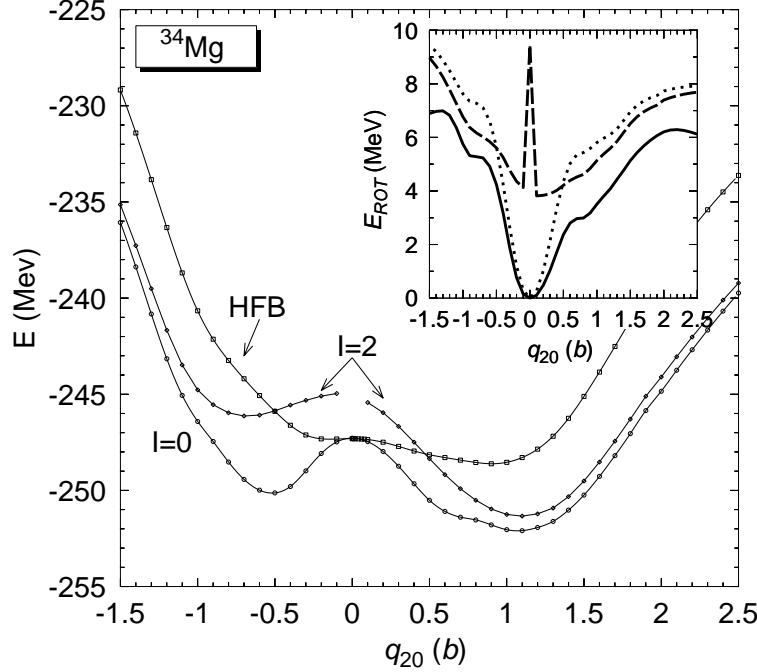


Fig. 1. The HFB and projected energies as a function of q_{20} for the nucleus ^{34}Mg . See text for further details.

in the evaluation of the density dependent term of the force in $E[\phi, \phi']$. In our case, this leads to the introduction of a density dependent term depending on $\bar{\rho}(\vec{r}, \beta) = \langle \phi | \hat{\rho} e^{-i\beta \hat{J}_y} | \phi \rangle / \langle \phi | e^{-i\beta \hat{J}_y} | \phi \rangle$. This density dependence seems to yield to bizarre consequences like having a non-hermitian and non rotationally invariant hamiltonian. These apparent inconsistencies can be overcome if we think of a density dependent force, not as an operator to be added to the kinetic energy in order to obtain a hamiltonian, but rather as a device to get energy functionals like $E[\phi]$ and $E[\phi, \phi']$ with the property of yielding an energy that is a real quantity and independent of the orientation of the reference frame. The density dependence just mentioned fulfills these two requirements as can be readily checked. In addition, when the intrinsic wave function is strongly deformed and the Kamlah expansion can be used to obtain an approximate expression for the projected energy (the cranking model) the above density dependence yields the correct expression for the angular velocity ω including the “rearrangement” term [24]. A more elaborated argumentation in favor of the density dependence just mentioned will be given elsewhere.

As an example of the results obtained we show in Fig. 1 the HFB and projected energies as a function of q_{20} for the nucleus ^{34}Mg . In contrast with the HFB result, the $I = 0$ energy surface shows two pronounced minima in the prolate and oblate side which are rather close to each other in energy being the prolate minimum slightly deeper than the oblate one. Therefore, it is difficult to assign a given character to the $I = 0$ state until a configuration mixing calculation is performed, although it is very likely that the predominant configuration

for the $I = 0$ state is going to be the prolate one. For $I = 2$ there is a well developed prolate minimum. Let us also mention that for configurations with a q_{20} value close to zero (i.e. close to the spherical configuration $q_{20} = 0$ which is a pure $I = 0$ state) it is very difficult to compute the $I = 2$ projected energy due to numerical instabilities related to the smallness of $\langle \phi(q_{20}) | \hat{P}_{00}^I | \phi(q_{20}) \rangle$.

In the inset of Fig. 1 we have plotted the energy difference $E_{ROT}(I) = E_{HFB} - E_I$ as a function of q_{20} for $I = 0$ (full line) in order to compare it with the rotational energy correction $E_{ROT}^{App} = \langle J_y^2 \rangle / \mathcal{J}_Y$ often used in mean field calculations (dashed line). The Yoccoz moment of inertia \mathcal{J}_Y has been computed, as it is usually done, in an approximate way by neglecting the two body quasi-particle interaction term of the hamiltonian (the same kind of approximation yields to the Inglis-Belyaev moment of inertia instead of the Thouless-Valatin one). We notice that E_{ROT}^{App} agrees qualitatively well with $E_{ROT}(0)$ for q_{20} values greater than $100 fm^2$ and smaller than $-50 fm^2$ as expected: these are regions of strong deformation where the validity conditions for E_{ROT}^{App} to be a good approximation to E_{ROT} (Kamlah expansion) are satisfied. On the other hand, the behavior of E_{ROT}^{App} is completely wrong in the inner region. One prescription to extend the rotational formula to weakly deformed states is the one of [25] based on results with the Nilsson model. The prescription multiplies E_{ROT}^{App} by a function of $\langle J_y^2 \rangle$ with the property of going to zero (one) for $\langle J_y^2 \rangle$ going to zero (infinity). The resulting rotational energy is also depicted in the inset of Fig. 1 (dotted line) and, although the qualitative agreement with the exact result improves somewhat, the quantitative one is far from satisfactory in the nucleus considered. The rotational energy correction formula is based on the assumption that the quantity $h(\beta) = \langle \hat{H} e^{-i\beta \hat{J}_y} \rangle / \langle e^{-i\beta \hat{J}_y} \rangle$ can be very well approximated by a quadratic function $h(\beta) \approx h(0) + \frac{1}{2} h''(0) \beta^2$ where $h''(0)$ is related to the exact Yoccoz moment of inertia by the expression $\mathcal{J}_Y = - \langle \hat{J}_y^2 \rangle^2 / h''(0)$. It is well known that this assumption is justified for deformed heavy nuclei. However, we have checked that it is not the case for the nuclei studied here even for the largest deformations considered. Therefore, we conclude that the exact restoration of the rotational symmetry is fundamental for a qualitative and quantitative description of the rotational energies in these light nuclei.

The main outcomes of the calculation are summarized in Fig. 2 where we show, on the left hand side panel, the HFB potential energy surfaces for Mg and Si isotopes as a function of the mass quadrupole moment. These surfaces have been shifted accordingly to fit them in the plot. We observe that only in the nuclei ^{34}Mg and ^{38}Si we obtain a prolate minimum at β_2 deformations of 0.4 and 0.35 respectively. For the other nuclei, the minimum corresponds to the spherical configuration. For all the nuclei considered the energy curves are very flat around the corresponding minimum indicating that further correlations can substantially modify the energy landscape and therefore the conclusions

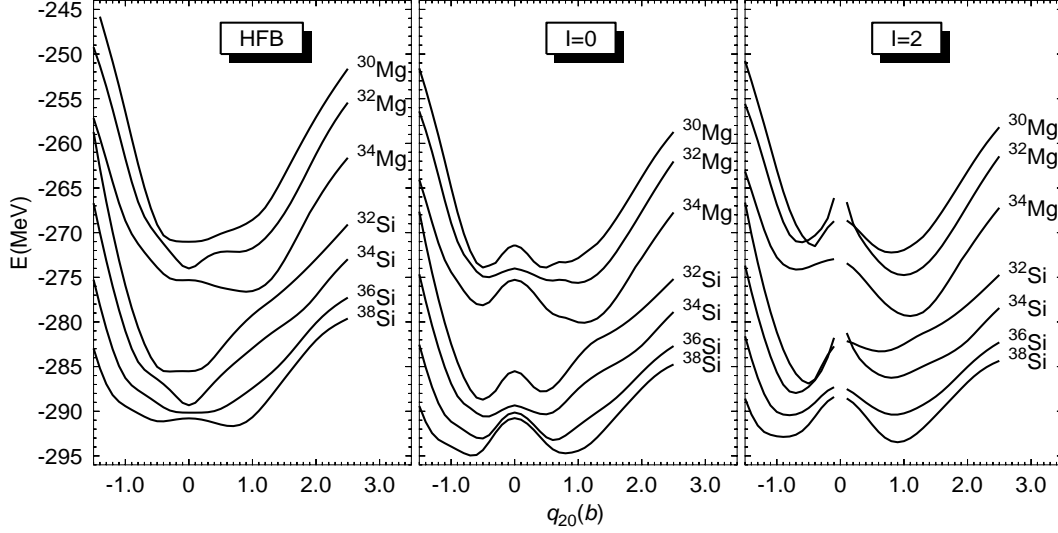


Fig. 2. HFB (left), angular momentum projected $I = 0$ (middle) and $I = 2$ (right) collective potential energy surfaces for the nuclei $^{30,32,34}\text{Mg}$ and $^{32,34,36,38}\text{Si}$. All the curves have been shifted by the same amount for each nucleus in all the three cases in order to fit them in a single plot. The energy shifts are -36, -30, and -28 MeV for $^{30,32,34}\text{Mg}$ and -23, -13 and -6 MeV for $^{32,34,36}\text{Si}$ respectively. The range of quadrupole moments considered roughly correspond to a β_2 range from -0.5 to 0.85.

obtained from the raw HFB results.

On the middle and right hand side panels of Fig. 2 we show the angular momentum projected $I = 0$ and $I = 2$ potential energy surfaces for all the nuclei considered. These surfaces have also been shifted to fit them in the plot. For $I = 0$, apart from the nucleus ^{34}Mg that shows a rather clear prolate minimum, the general trend for the ground state is to show shape coexistence. For $I = 2$ we have prolate minima for $^{32-34}\text{Mg}$ and oblate minima for $^{32-34}\text{Si}$ whereas the other nuclei are examples of shape coexistent structures. The results just shown indicate that, for a quantitative description of the ground and 2^+ states in all these nuclei, a configuration mixing calculation (GCM) using the mass quadrupole moment as generating coordinate is needed. In spite of this, we present in Table 1 the $0^+ - 2^+$ energy differences for the four possible configurations with the 0^+ in the prolate (P) or oblate (O) minimum and the 2^+ also in the P or O minimum. The energies written in boldface correspond to the predictions obtained by strictly using the criterion of the absolute minimum of $E_I(q_{20})$ to assign the 0^+ and 2^+ states. Comparison of these predictions with the experimental results indicates a reasonable agreement except for ^{36}Si . The inclusion of configuration mixing will presumably improve the agreement as it always yields to a mixed configuration with an energy lower than the energies of the states being mixed. Therefore, if the 0^+ configurations strongly mix (shape coexistence) but the 2^+ ones do not (there is a well established minima) the $0^+ - 2^+$ energy difference will increase whereas it will decrease if the opposite situation takes place. On the other hand, if configuration mix-

Table 1

Excitation energies, in MeV, for the 2^+ states. The four possible combinations are shown. The numbers in boldface indicate the configuration where the 0^+ and the 2^+ correspond to the absolute minimum of the projected energy surface. The experimental data are taken from [4] (Si) and from [2] (Mg).

	$(0_P^+ - 2_P^+)$	$(0_O^+ - 2_P^+)$	$(0_P^+ - 2_O^+)$	$(0_O^+ - 2_O^+)$	Exp
^{30}Mg	1.683	1.681	2.391	2.388	
^{32}Mg	0.873	0.235	4.546	3.909	0.885
^{34}Mg	0.753	-1.206	5.960	4.000	
^{32}Si	4.475	5.408	0.869	1.803	1.941
^{34}Si	4.088	4.324	2.383	2.619	3.327
^{36}Si	2.845	2.670	2.778	2.603	1.399
^{38}Si	1.238	1.481	1.837	2.080	1.084

ing is important for both the 0^+ and 2^+ states anything can happen to the excitation energy. Therefore, we expect that configuration mixing is going to increase the excitation energies in all cases except in ^{30}Mg and $^{36,38}\text{Si}$ where the behavior is unpredictable. In Table 2 we present the results obtained for the $B(E2, 0^+ \rightarrow 2^+)$ transition probabilities for the four possible combinations. As in the previous table, the results obtained by choosing for the 0^+ and 2^+ states the ones corresponding to the absolute minima of the projected energies are written in boldface. For the nuclei ^{32}Mg and ^{34}Mg we obtain very collective values for the $B(E2)$ which, in the case of ^{32}Mg , are in rather good agreement with the experiment. For both nuclei, we expect a contamination of the ground state wave function by the oblate 0^+ state that will yield to a reduction of the $B(E2)$ values (see column two for the $B(E2, 0_O^+ \rightarrow 2_P^+)$) that will bring the theoretical predictions in closer agreement with the experimental data. For the ^{32}Si , ^{34}Si and ^{38}Si isotopes we underestimate the $B(E2)$ values but, presumably, admixtures of the $0_P^+ \rightarrow 2_P^+$ transition will help to bring the theoretical results in closer agreement with the experiment, specially for the ^{38}Si nucleus. Concerning ^{36}Si we can only conclude that a strong $0_P^+ \rightarrow 2_P^+$ component has to be present in the evaluation of the $B(E2)$.

In Table 3 the HFB and projected ground state energies for the nuclei under consideration are shown and compared to the experimental data taken from [26]. The inclusion of the zero point energy stemming from the restoration of the rotational symmetry clearly improves the theoretical description of the binding energies.

In conclusion, we have computed several properties of neutron rich Mg and Si isotopes using the HFB theory and exact angular momentum projection. In the calculations the finite range density dependent Gogny force has been

Table 2

Transition probabilities $B(E2, 0^+ \rightarrow 2^+)$ in $e^2 fm^4$ between different configurations in $^{30,32,34}Mg$ and $^{32,34,36,38}Si$. As in the previous table O (P) stands for the oblate (prolate) configuration. The experimental data is taken from [4] (Si) and from [3] (Mg).

	$0_P^+ \rightarrow 2_P^+$	$0_O^+ \rightarrow 2_P^+$	$0_P^+ \rightarrow 2_O^+$	$0_O^+ \rightarrow 2_O^+$	Exp.
^{30}Mg	182.11	39.44	0.88	8.38	
^{32}Mg	593.24	15.53	2.26	6.52	454±78
^{34}Mg	549.21	14.74	2.66	10.51	
^{32}Si	402.09	54.19	4.26	50.71	113±33
^{34}Si	227.18	62.51	6.81	39.16	85±33
^{36}Si	232.22	45.05	6.43	28.31	193±59
^{38}Si	418.91	35.18	4.43	69.80	193±71

Table 3

Ground state energies in MeV as compared to the experimental results. The quantities $\delta E_{I=0} = E_{Exp} - E_{I=0} - E_{C.E.}$ and $\delta E_{HFB} = E_{Exp} - E_{HFB} - E_{C.E.}$ are also presented. The quantity $E_{C.E.}$ stands for the HFB Coulomb exchange energy computed in the Slater approximation. The experimental data are taken from [26].

	E_{HFB}	$E_{I=0}$	$E_{C.E.}$	E_{Exp}	$\delta E_{I=0}$	δE_{HFB}
^{30}Mg	-235.01	-237.90	-4.29	-241.63	0.56	-2.33
^{32}Mg	-244.00	-245.62	-4.22	-249.68	0.16	-1.46
^{34}Mg	-248.61	-252.09	-4.21	-256.58	-0.28	-3.76
^{32}Si	-262.55	-265.70	-5.13	-271.41	-0.58	-3.73
^{34}Si	-276.32	-277.59	-5.06	-283.42	-0.77	-2.04
^{36}Si	-284.15	-287.22	-5.04	-292.01	0.25	-2.82
^{38}Si	-291.66	-294.95	-4.98	-299.50	0.43	-2.86

used. The results for the excitation energies $0^+ - 2^+$ and $B(E2, 0^+ \rightarrow 2^+)$ transition probabilities obtained from the angular momentum projected wave functions are in reasonable agreement with the experiment. The analysis of the projected energy surfaces and also the discrepancies found between theory and experiment indicate that configuration mixing is an important ingredient in these nuclei. Work is in progress in order to incorporate such configuration mixing.

One of us (R. R.-G.) kindly acknowledges the financial support received from the Spanish Instituto de Cooperacion Iberoamericana (ICI). This work has been supported in part by the DGICYT (Spain) under project PB97/0023.

References

- [1] C. Thibault et al., Phys. Rev. **C12** (1975) 644.
- [2] D. Guillemaud-Mueller et al., Nucl. Phys. **A426** (1984) 37.
- [3] T. Motobayashi et al., Phys. Lett. **B346** (1995) 9.
- [4] R. W. Ibbotson et al., Phys. Rev. Lett. **80** (1998) 2081.
- [5] D. Habs et al., Nucl. Phys. **A616** (1997) 29c.
- [6] X. Campi, H. Flocard, A.K. Kerman and S. Koonin, Nucl. Phys. **A251** (1975) 193.
- [7] M. Barranco and R.J. Lombard, Phys. Lett. **B78** (1978) 542.
- [8] R. Bengtsson, P. Möller, J.R. Nix and J.-y. Zhang, Phys. Scr. **29** (1984) 402.
- [9] Z. Ren, Z.Y. Zhu, Y.H. Cai and G. Xu., Phys. Lett. **B380** (1996) 241.
- [10] G. A. Lalazissis, A.R. Farhan and M.M. Sharma, Nucl. Phys. **A628** (1998) 221.
- [11] J. Terasaki, H. Flocard, P.-H. Heenen and P. Bonche, Nucl. Phys. **A621** (1997) 706.
- [12] J. F. Berger et al., Inst. Phys. Conf. Ser. **132** (1993) 487.
- [13] A. Watt, M.H. Storm and R.R. Whitehead, J. Phys. **G7** (1981) L145.
- [14] A. Poves and J. Retamosa, Phys. Lett. **B184** (1987) 311; Nucl. Phys. **A571** (1994) 221.
- [15] P.-G. Reinhard et al., Phys. Rev. **C60** (1999), 014316.
- [16] J.F. Berger, M. Girod and D. Gogny, Nucl. Phys. **A428** (1984) 23c.
- [17] J. Dechargé and D. Gogny, Phys. Rev. **C21** (1980) 1568.
- [18] L. M. Robledo, Phys. Rev. **C50** (1994) 2874; J.L. Egido, L.M. Robledo and Y. Sun, Nucl. Phys. **A560** (1993) 253.
- [19] P. Ring and P. Schuck, *The Nuclear Many Body Problem* (Springer, Berlin, 1980).
- [20] K. Hara and Y. Sun, Int. J. Mod. Phys. **E4** (1995) 637.
- [21] R. G. Nazmitdinov, L.M. Robledo, P. Ring and J.L. Egido, Nucl. Phys. **A596** (1996) 53.
- [22] K. Hara, A. Hayashi and P. Ring, Nucl. Phys. **A385** (1982) 14.
- [23] P. Bonche, J. Dobaczewski, H. Flocard, P. -H. Heenen and J. Meyer, Nucl. Phys. **A510** (1990) 466.

- [24] A. Valor, J.L. Egido and L.M. Robledo, Phys. Rev. **C53** (1996) 172; Phys. Lett. **B392** (1997) 249.
- [25] P.-G. Reinhard and K. Goeke, Rep. Prog. Phys. **50** (1987) 1.
- [26] G. Audi and A.H. Wapstra, Nucl. Phys. **A595** (1995) 409.